Magnetic Resonance in Medicine 49:638–645 (2003)

Is Multicomponent T_2 a Good Measure of Myelin Content in Peripheral Nerve?

Stephanie Webb,[1] Catherine A. Munro,[2] Rajiv Midha,[2,3] and Greg J. Stanisz[1,4]*

Multicomponent T_2 relaxation of normal and injured rat sciatic nerve was measured. The T_2 relaxation was multiexponential, indicating the multicompartmental nature of T_2 decay in nerve tissue. The size of the short, observed T_2 component correlated very well with quantitative assessment of myelin using computer-assisted histopathological image analysis of myelin. Specifically, the size of the short T_2 component reflected the processes of myelin loss and remyelination accompanying Wallerian degeneration and regeneration following trauma. However, it represented all myelin present in the sample and did not distinguish between intact myelin and myelin debris. Other changes in T_2 spectra were also observed and could be correlated with axonal loss and inflammation. The study also questions the validity of previously offered interpretations of T_2 spectra of nerve. Magn Reson Med 49:638–645, 2003.

Key words: axonal loss; histomorphometry; inflammation; MRI; myelin; sciatic nerve; T_2 relaxation; Wallerian degeneration

Normal neural tissues have been imaged with reasonable accuracy and anatomical detail in all parts of the body: peripheral nerve (1–3), optic nerve (1,4), spinal cord (3,5), and nerve roots (5). In severe trauma, MR neurography has identified nerve discontinuity, verifying the need for surgical repair (6). Hyperintensity of T_2-weighted MR images correlates well with nerve compression in entrapment neuropathies (7). However, current MRI techniques are not capable of discriminating whether an injured nerve has the potential to spontaneously regenerate or whether surgical intervention is required to promote recovery. Application of quantitative MRI techniques that correlate MR signal characteristics with changes in tissue microstructure have exhibited utility in evaluating various nervous system pathologies (8–12). Myelination is commonly used as an indicator of nerve health. T_2 relaxation has been qualitatively correlated with myelin content (13,14), but to our knowledge a quantitative correlation has not previously been reported. The development of quantitative T_2 measurements for assessing myelin would be a very useful tool for physicians assessing nerve damage and having to make a decision regarding the necessity of intervention or the effectiveness of treatment. Quantitative T_2 and magnetization transfer (MT) measurements have been proposed as suitable methods for myelin evaluation (8,10,11,13). Both methods are capable of measuring certain aspects of water molecular dynamics; however, it has been proposed that multicomponent T_2 could provide a more direct measure of myelin in the nervous system (11). Multicomponent T_2 spectra have been suggested for quantitative measurements of nerve (if exchange between compartments can be neglected), and the short T_2 component has been identified with myelin-associated water (9,13–16). The goal of this study was to assess whether multicomponent T_2 is a quantitative measure of myelin content in peripheral nerve. In particular, we examined whether the short T_2 component correlates with myelin content in normal and injured nerve. In order to evaluate this correlation, we used an animal model of nerve injury and measured T_2 in vitro and performed quantitative histomorphometry on nerve samples.

We used a rat model of nerve injury in which Wallerian degeneration (WD) was induced by crushing or cutting nerves (17) to explore the ability of multicomponent T_2 measurements to detect nerve injury and to distinguish between nerve that is degenerating and nerve that was injured yet regenerating. In this model of WD a transection of the rat sciatic nerve leads to irreversible degeneration, whereas a crushed nerve undergoes initial degeneration followed by subsequent regeneration (18,19).

First, a conventional histomorphometry approach was used to evaluate intact myelin sheaths. Next, a modified histomorphometry technique based on color intensity was employed to measure all myelin, including both healthy and degenerating nerve fibers and myelin debris.

METHODS

Inbred, adult male Lewis rats (250–300 g, 10 weeks old) were obtained from Harlan Sprague Dawley (Indianapolis, IN) and were housed in a standard animal facility with 12-hr on/off light conditions. All animals were acclimated prior to surgery and allowed standard rat chow and water ad libitum. All experiments and animal interventions adhered to Canadian Council on Animal Care guidelines. The anesthesia used in all cases consisted of an intramuscular injection of 10 mg/kg xylazine (20 mg/mL; Bayer, Etobicoke, ON) and 100 mg/kg ketamine hydrochloride (0.1 mL / 100 g Rogarestic; Rogra-STB, Montreal, QC) into the lumbar paraspinal musculature. All surgical procedures employed standard microsurgical techniques using an operating microscope (Wild M651; Wild Leitz, Willowdale, ON). Following anesthesia induction the sciatic nerves were exposed via bilateral gluteal and posterior

[1]Imaging Research, Sunnybrook & Women's College Health Sciences Centre, Toronto, Canada.

[2]Neuroscience Research and Division of Neurosurgery, Sunnybrook & Women's College Health Sciences Centre, Toronto, Canada.

[3]Department of Surgery, University of Toronto, Toronto, Canada.

[4]Department of Medical Biophysics, University of Toronto, Toronto, Canada.

Grant sponsor: Canadian Institutes of Health Research; Grant number: MOP 57894.

*Correspondence to: Greg J. Stanisz, Ph.D., Imaging Research, Sunnybrook & Women's College Health Sciences Centre, S654, 2075 Bayview Avenue, Toronto, ON M4N 3M5, Canada.

Received 28 February 2002; revised 31 October 2002; accepted 6 November 2002.

DOI 10.1002/mrm.10411
Published online in Wiley InterScience (www.interscience.wiley.com).

thigh incisions. One sciatic nerve was crushed using a #4 Jeweler's forceps for 1 min. The injury caused transection of the axons but left the perineurium intact. The site of crush was marked with a 5-0 suture tied in surrounding muscle. The other sciatic nerve was cut and the proximal nerve stump was ligated with 5-0 suture to prevent reinnervation of the distal nerve stump. Overlying muscles were sutured with 3-0 absorbable sutures and the skin incisions were then approximated with continuous 3-0 silk sutures.

We used the generally accepted rat model of WD, measuring MR properties of the portions of the nerves distal to the inflicted injury. Cutting the nerve and ligating the proximal stump causes irreversible degeneration in the portion of the nerve distal to the injury. The distal segment of the crushed nerve undergoes initial degeneration followed by regeneration (20). Proximal portions of the nerve remain relatively unaffected.

At the study endpoint (1, 2, 3, 4, and 6 weeks postinjury), the animals were anesthetized as above. Three animals were used for each time point, as well as three normal controls for a total of 18 animals. Under the operating microscope, the nerves were reexposed and the nerve tissue harvested. Four samples, each ~1 cm in length, were collected from each rat: the distal stump of the cut nerve, the proximal stump of the cut nerve, a distal sample of the crushed nerve taken from between the injury site and the branching point of the tibial and peroneal nerves, and a proximal sample of the crushed nerve. Control samples from uninjured rats were removed from locations representative of the distal and proximal regions.

All samples were placed in nonprotonated, MR-compatible fluid (Fluorinert; 3M, London, ON) to avoid dehydration and to reduce susceptibility effects. The multicomponent T_2 relaxation was immediately measured to probe the MR characteristics of neural tissue at different stages of degeneration and regeneration. In addition, histology samples were collected at the proximal and distal ends of the distal nerve sample. Samples were fixed by immersion in Universal fixative (40% formalin, 25% glutaraldehyde). The more distal histology samples (33 samples total) were used for quantitative histomorphometric analysis. The histology samples were postfixed with osmium tetroxide and embedded in epon-araldite and underwent sectioning on an ultramicrotome (Sorvall MT6000, Kendro, Asheville, NC, and Reichert-Jung Ultracut E, Leica Microsystems, Germany). Toluidine blue was used to stain 1-μm thick cross-sections for light microscopy. The proximal histology samples (which were actually distal to the injury site) were taken to ensure that the inflicted cut or crush had indeed caused degeneration in the nerve distal to the injury site. Histological evidence of WD in the proximal histology samples was evidence that the injury had resulted in WD and upon reexposure of the nerve the injury site had been correctly identified and the distal MR sample was in fact taken from tissue distal to the injury.

All MR measurements were performed at 20°C and 1.5 T on a 20 cm bore superconducting magnet (Nalorac Cryogenics, Martinez, CA) controlled by an SMIS spectroscopy console (SMIS, Surrey, UK). Rectangular RF pulses were amplified by an RF amplifier (Model 3205; American Microwave Technology, Brea, CA). T_2 was measured using a Carr-Purcell-Meiboom-Gill (CPMG) (21,22) sequence with TE/TR=1/10,000 ms, 2500 even echoes sampled, and 200 averages, resulting in an average signal-to-noise ratio (SNR) of approximately 3000. Spectral width was 200 kHz. The average duration of the π pulse was 12 μs. The T_2 decay curves were non-monoexponential, implying tissue compartmentalization, and were thus fitted to a multicomponent T_2 model in which the relaxation of each T_2 component has a Gaussian distribution on a logarithmic time scale (23). The Gaussian model was found to provide better separation of the T_2 peaks than the commonly used nonnegative least squares (NNLS) method (24), yet guaranteed approximately the same value of χ^2 and resulted in similar T_2 spectra. Repeated T_2 measurements of a single sample were used to determine that a minimum SNR of 500 was required for assessment of the amplitudes and positions of all three T_2 components with 5% precision.

Computer-assisted image analysis has been used in studies of nerve histology to increase the speed and reliability of analysis and to reduce observer bias (25). Computer-assisted image analysis was performed on the Toluidine blue-stained samples using image analysis software (Image-Pro Plus 4.5, Media Cybernetics, Silver Spring, MD). Histomorphometric studies to evaluate myelin content of each nerve section were performed on randomly selected, representative fields of known area (18,940 μm^2) at 630× magnification on a light microscope. Several samples were also evaluated at 1000× magnification. The representative fields were selected from the largest fascicle in each sample. The number of fields (three to five) evaluated depended on the total cross sectional sample area and was selected such that total area evaluated was approximately 25% of total sample area. Images were captured for further analysis, which involved a three-step approach modeled on the segmentation, recognition, and measurement method of Romero et al. (25). In the first step, thresholding, the goal was to maximize contrast between myelin and the background, while retaining all relevant information. In the second step, filtering was performed to remove "speck"-type artifacts and improve object separation. This was accomplished via application of an "erosion" filter (reduced the edge of all dark objects by one pixel) followed by a "dilation" filter (increased the edge of dark objects by one pixel). In the final measurement step, the user identified a color intensity value corresponding to myelin (Toluidine blue stains myelin dark blue), and the software selected all myelin and calculated the cross-sectional myelin area. The selected color intensity value varied from image to image due to variations in intensity of the Toluidine blue staining. An initial value was selected by the software based on the color histogram of the image, which was used to classify pixels as either "light" or "dark." A trained observer then manually adjusted the cut-off value for improved accuracy. The evaluation took into account intact myelin sheaths, as well as myelin present in the form of WD profiles or disrupted myelin sheaths. The myelin content was calculated as a percentage of total sampled area. The color-intensity-based technique described above will be referred to as HM2. The color-intensity-based results were compared to the results obtained using a conventional histomorphometry technique (referred to as HM1). In this method (HM1), the thresholding

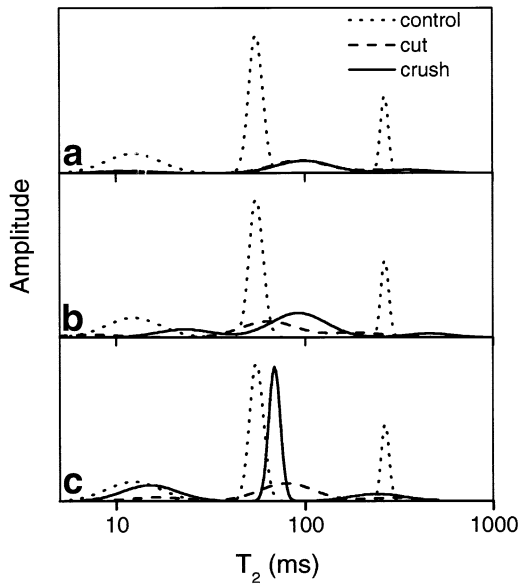

FIG. 1. A multicomponent T_2 spectrum of normal (control) nerve shows three distinct peaks. Representative spectra illustrate the characteristic changes observed following injury. Cut and crushed nerve samples taken from a single animal at 2 weeks after injury exhibit a short T_2 component reduced in sized compared to a normal control (**a**). Partial recovery of the short T_2 component is observed at 4 weeks after injury (**b**). After 6 weeks, T_2 component size is comparable in crushed and normal nerve, while component size in cut nerve remains reduced (**c**).

and filtering steps were performed as in HM2. Next, trained observers identified healthy fibers based on morphology and the software was used to calculate myelin cross-sectional area of these healthy fibers only. The conventional histomorphometry methodology reflects the interests of pathologists, who typically wish to quantify only viable nerve fibers.

Although 630× magnification was sufficient for resolution of the relevant structures in almost all cases, in a few samples with particularly dark staining it was very difficult to accurately distinguish myelin from adjacent Schwann cells. Evaluation of these samples at 1000× magnification resulted in a more accurate identification of myelin. Several other slides, less darkly stained, were also evaluated at 1000× and the values of HM1 and HM2 obtained were found to be consistent with the results at 630×.

RESULTS

The Gaussian fitting procedure yielded values for the T_2 spectrum position, width, amplitude, and relative size of each component. Typical T_2 spectra for injured nerve at three different time points after injury compared to normal (uninjured) nerve are shown in Fig. 1. The T_2 spectrum of normal nerve (dotted line) shows three well-distinguished components, centered at short, intermediate, and long values of T_2:

- A short T_2 component at 19 ± 1 ms (average and standard error of the mean for three samples) represented 32 ± 5% of the total curve area.
- An intermediate T_2 component at 58 ± 6 ms with size 47 ± 3%.
- A long T_2 component at 219 ± 27 ms and size 21 ± 3%.

The T_2 spectra of the distal nerve samples collected at 1–6 weeks after injury were examined and found to be different than the spectra of normal nerve. Furthermore, these differences changed over time and the pattern of changes observed in the crushed nerves differed from that observed in the cut nerves. The T_2 spectra characteristics of the proximal portions of the injured nerves were very similar to those of uninjured nerves.

Figure 1 illustrates the pattern of changes seen in the spectra of injured nerves compared to normal nerves for representative samples (T_2 component parameter values for all samples at each time point are shown in Tables 1, 2). Following injury, the size of the short T_2 component decreased in both cut and crushed nerves. Two weeks after injury the size of the short T_2 component was similar in cut and crushed nerves (for the spectra shown, 14% and 12%, respectively). Four weeks after injury the size of the short component remained reduced in cut nerve, while in crushed nerve it increased (for the spectra shown, 11% and 22%, respectively). Subsequently, component size for

Table 1
T_2 Component Positions of Normal and Injured Nerve Samples

	Control samples			Injury type	Postinjury timepoints														
					1 week			2 weeks			3 weeks			4 weeks			6 weeks		
Short component position (ms)	18	20	19	crush	15	25	18	12	11	18	23	9	10	23	20	21	13	15	15
				cut	18	23	25	11	10	25	9	9	19	7	16	30	19	17	12
Intermediate component position (ms)	51	52	70	crush	88	106	82	99	94	98	97	77	83	92	74	89	66	69	52
				cut	93	96	118	94	77	112	69	67	87	64	77	108	82	80	72
Long component position (ms)	201	185	272	crush	252	380	249	351	301	329	302	246	284	458	173	261	240	240	206
				cut	291	324	480	272	220	410	191	173	248	187	213	487	389	296	212

T_2 spectra parameter values (T_2 position) for distal cut and crush nerve samples at 1–6 weeks after injury and for normal controls. Each column represents results for a different animal, including three animals for each time point postinjury and three normal control samples. For greater readability, error estimates are not shown, but are at most 5%.

Table 2
T_2 Component Sizes of Normal and Injured Nerve Samples

	Control samples			Injury type	Postinjury timepoints														
					1 week			2 weeks			3 weeks			4 weeks			6 weeks		
Short component area (%)	25	31	41	crush	23	26	29	12	12	24	27	11	14	22	30	32	25	31	34
				cut	25	30	26	14	13	24	11	9	17	11	20[a]	25[a]	19	15	21
Intermediate component area (%)	53	44	44	crush	65	66	60	69	65	66	62	65	70	69	56	62	68	55	57
				cut	67	63	65	69	66	65	61	66	54	70	62	65	70	71	69
Long component area (%)	22	25	15	crush	12	7	11	18	22	9	11	24	16	8	14	6	7	14	8
				cut	8	7	9	18	21	10	28	25	29	20	18	10	11	13	10

[a]Two samples had an unusually large short T_2 component. These samples displayed a particularly steep slope at the beginning of the T_2 decay curve; the Gaussian model yielded an unusually large short T_2 spectrum component. NNLS analysis of these samples (with no restriction on the number of components) indicated two components occurring under 20 ms; a very short component at approximately 0–5 ms with large amplitude and a second short component at approximately 15–20 ms. The very short component may be an artifact of inferior SNR or a nonmyelin component. Thus, the unusually large size of the short T_2 component of these samples may be an overestimation of myelin content.

crushed nerves continued to increase, and by 6 weeks reached values in the range of normal nerves (30 ± 3%). This recovery was not observed in the cut nerves, with short component size remaining depressed at all time points. Short T_2 component position and width did not significantly change.

Positions of the intermediate and long T_2 components increased in both cut and crushed nerve following injury and remained greater than in normal nerve through 4 weeks postinjury, returning to relatively normal T_2 times by 6 weeks. Intermediate component size increased slightly after injury and remained elevated at all time points. Changes in long T_2 component size did not follow a consistent pattern.

In order to determine whether size of the short T_2 component was quantitatively correlated with myelin content, histomorphometric studies of nerve pathology sections were performed. Figure 2 shows representative histopathology sections of normal nerve, as well as cut nerve and crushed nerve 3 weeks after injury. Normal nerve (Fig. 2a) shows densely packed nerve fibers consisting of axons sheathed in a uniformly thick layer of myelin. The histopathology sections of the distal nerve samples collected at 1–6 weeks after injury were examined and found to exhibit signs of degeneration, including loss of myelination, WD profiles, and inflammatory cells. Characteristic changes were observed over time and the pattern of changes observed in the crushed nerves differed from that observed in the cut nerves. In cut nerves (Fig. 2b), substantial changes were observed at 3 weeks postinjury. The structural arrangement of nerve fibers and myelin integrity was lost. A large number of onion-like WD profiles were visible. Active Schwann cells and inflammatory cells were present. The ratio of extracellular matrix space to neural tissue increased. In crushed nerve (Fig. 2c), evidence of degeneration similar to what is seen in cut nerve was apparent, but signs of regeneration are also observed as early as 3 weeks after injury. Sprouting of a single regenerating axon gives rise to several small-diameter axons that are myelinated by Schwann cells. By 6 weeks postinjury, well-myelinated axons indicated regeneration of the crushed nerve. In the cut nerve, the lack of myelinated axons indicated complete degeneration. As expected, the histopathology sections of the proximal portions of the cut and crushed nerves resembled those of normal nerve.

Two different techniques, as detailed in the Methods section, were used to measure the myelin content of distal nerve tissue samples. Figure 3a shows a typical section of injured nerve stained with Toluidine blue for identification of myelin. Figure 3b shows the conventional morphometric technique (HM1) for evaluation of myelin in peripheral nerve samples, based on the measurement of intact, mature nerve fibers. Myelin present in the form of WD profiles or disrupted myelin sheaths is not accounted for by this method. Finally, Fig. 3c shows all myelin present in the sample, based on an algorithm (HM2) that selects objects for measurement based on color intensity (of myelin staining). The histomorphometry technique illustrated here allowed us to measure structural features of normal and damaged neural tissue, including: healthy (intact) nerve fibers, degenerating fibers, myelin debris, and regenerating fibers and to quantitatively assess the extracellular matrix space.

Tables 1, 2, and 3 summarize Gaussian T_2 analysis of the MRI data and histomorphometry results for all measured samples. Different biological rates of nerve degeneration and regeneration render correlation of MR parameter values with time after injury inappropriate. However, the size of the T_2 component correlates well with the myelin content evaluated using color image analysis (HM2).

Figure 4 is a plot of short T_2 component size vs. myelin content assessed by histomorphometry. Figure 4a shows results of conventional histomorphometric evaluation of myelin (HM1). Figure 4b shows myelin content as determined using the color-intensity-based method (HM2). Three of the data points plotted in Fig. 4 were evaluated at 1000× magnification. For these samples, unusually dark staining resulted in low contrast between myelin and the background, making it extremely difficult to separate myelin from the background at 630× magnification.

Analysis of Fig. 4 and Tables 1–3 reveals that:

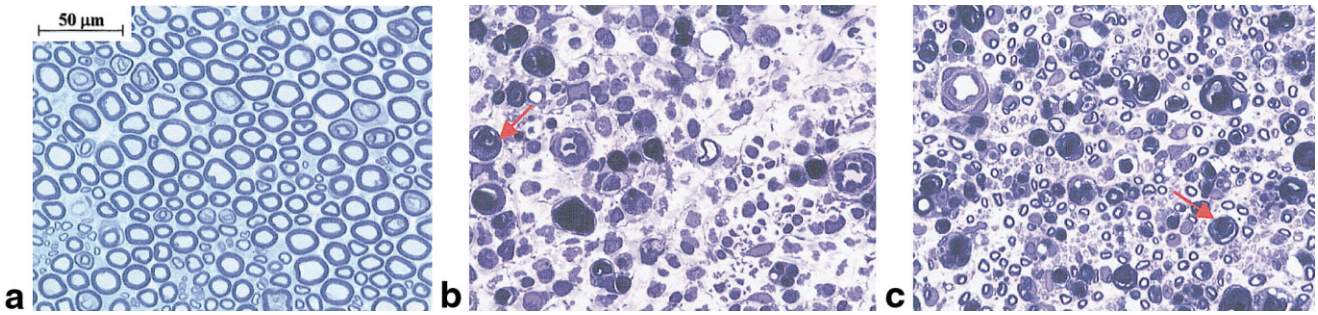

FIG. 2. Representative histopathology sections of normal nerve (**a**), cut nerve 3 weeks after injury (**b**), and crushed nerve 3 weeks after injury (**c**) at 630× magnification (before reduction). A number of differences are evident between normal and injured nerve samples. Healthy nerve (**a**) is characterized by closely packed, well-myelinated axons with relatively uniformly circular cross sections. The sections of injured nerve (**b,c**) show a loss of structure, large onion-like Wallerian degeneration profiles (arrows), and influx of inflammatory cells. In the crushed nerve (**c**), small newly (and thinly) myelinated axons indicate regeneration.

- HM1 (Fig. 4a) is 2% or less for all cut nerve samples as well as for crushed nerve samples one week after injury. Although some fields may contain a few normal fibers, their area is negligible compared to the field size.
- Correlation between short T_2 component size and HM1 is low ($R = 0.59$, $P < 0.001$). HM1 and short T_2 component size are in reasonable agreement for normal controls and for crushed nerve samples at later stages of regeneration (4–6 weeks postinjury). However, short T_2 component size does not correlate well with HM1 of the degenerating nerve samples (cut nerve samples at all time points and crushed nerve samples at 1–3 weeks after injury).
- Short T_2 component size correlates better with the HM2 method ($R = 0.75$, $P < 0.0001$) whereby all the myelin is measured. There is a near one-to-one correspondence between short T_2 component size and HM2 for both degenerating and regenerating nerve samples (slope of linear fit is 0.7 ± 0.1), including cut and crushed samples at all time points postinjury as well as normal controls. These results suggest that the short T_2 component does in fact represent total myelin content (HM2) rather than exclusively healthy myelin content (HM1).
- Two samples in the upper left corner of Fig 4b had an unusually large short T_2 component. Preliminary experiments revealed that, although component separation was achieved with a minimum SNR of 500, the T_2 decay of some, but not all, samples with SNR in the 500–800 range was inadequately approximated by the Gaussian model. These samples displayed a particularly steep slope at the beginning of the T_2 decay curve; the Gaussian model yielded an unusually large short T_2 spectrum component. NNLS analysis of these samples (with no restriction on the number of components) indicated two components occurring under 20 ms; a very short component at approximately 0–5 ms with large amplitude and a second short component at approximately 15–20 ms. The very short component may be an artifact of inferior SNR or a non-myelin component. Thus, the unusually large size of the short T_2 component of these samples may be an overestimation of myelin content.

We also quantified the relative increase in cross-sectional area of the extracellular matrix (EM) as shown in Table 3. In normal nerve, $42 \pm 3\%$ is EM. Following injury, the percentage of total nerve area occupied by EM increases relative to the percentage of area occupied by nerve fibers in both cut and crushed nerve with the processes of WD. In cut nerve, EM area increases from $69 \pm 3\%$ 1 week postinjury to $81 \pm 3\%$ at 6 weeks postinjury, reflecting ongoing degeneration and axonal loss without

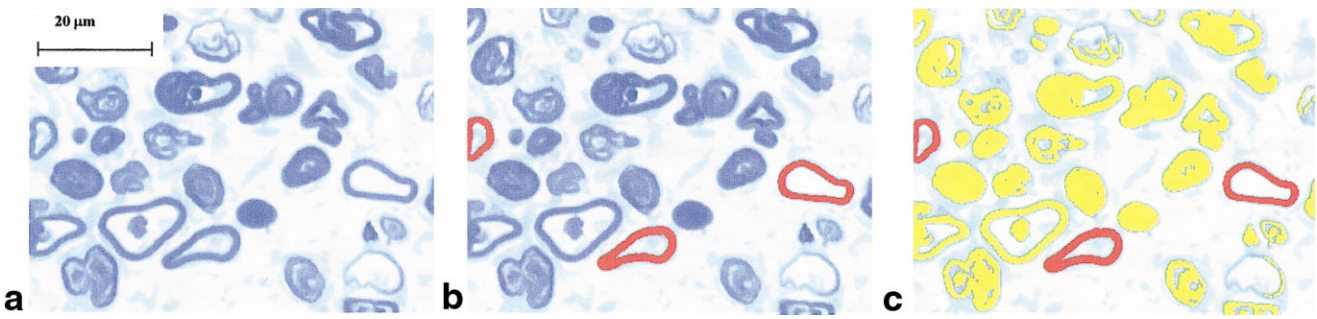

FIG. 3. Cut nerve one week after injury. Myelin was stained dark blue by Toluidine blue (**a**). A conventional histomorphometric method (HM1) was used to select healthy nerve fibers (red highlighting) for measurement (**b**). In contrast, a color-intensity-based method (HM2) identified all myelin in the sample, including healthy fibers (red), as well as degenerating myelin and myelin debris (yellow highlighting) (**c**).

Table 3
Histomorphometry Parameter Values for Normal and Injured Nerve Samples

	Control samples			Injury type	Postinjury timepoints														
					1 week			2 weeks			3 weeks			4 weeks			6 weeks		
Healthy myelin (HM1) (%)	34	41	39	crush	0	1	0	2[b]	4	0	3	2[b]	2[b]	11	11	9	15	18	20
				cut	2	1	1	0	0	0	0	0	0	0	0	0	0	0	0
Total myelin (HM2) (%)	34	41	39	crush	22	21	21	15[b]	15	20	22	10[b]	14[b]	18	22	23	23	27	32
				cut	21	26	29	14	17	21	14	12	14	15	7[a]	6[a]	22	12	19
Extracellular matrix area (%)	44	35	46	crush	68	68	77	51[b]	85	78	77	52[b]	78[b]	77	75	72	68	63	56
				cut	73	64	70	84	66	76	83	86	53	84	91	93	77	88	79

[a]See footnote a in Table 2.
[b]Three of the samples were evaluated at 1000× magnification. For these samples, unusually dark staining resulted in low contrast between myelin and the background, making it extremely difficult to separate myelin from the background at 630× magnification.

regeneration. EM area also increases in crushed nerve during the initial weeks following injury. It remains elevated through the fourth week after injury, while regeneration of nerve fibers is occurring, and fibers are small in diameter and dispersed through the EM. As regeneration progresses, the amount of neural tissue increases, and EM area decreases to 62 ± 3% by 6 weeks after injury.

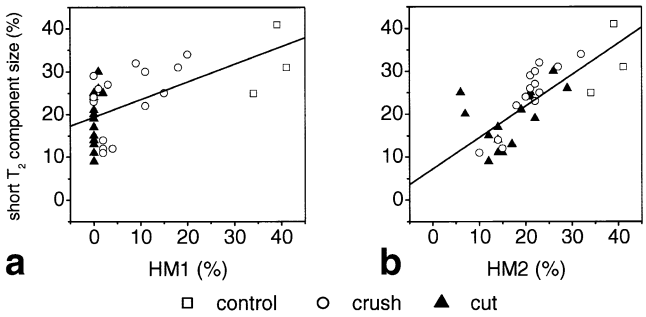

FIG. 4. Short T_2 component size is plotted against myelin content of nerves at different time points postinjury, as determined by two different methods. A conventional histomorphometric approach (HM1) evaluates healthy myelinated axons (**a**). A color-intensity-based approach (HM2) selects objects for measurement based on staining (**b**). Squares represent normal controls, circles represent crushed nerve samples, triangles represent cut nerve samples. A linear fit to the HM1 data (plotted as a solid line) yields a slope of 0.4 ± 0.1, R = 0.59, $P <$ 0.001. Although HM1 and component size of normal controls and regenerating samples (crushed nerves, 4–6 weeks postinjury) are in reasonable agreement, short T_2 component size does not correlate well with HM1 of the degenerating nerve samples (cut nerve samples and crushed nerve samples at 1–3 weeks after injury). Short T_2 component size correlates better with the HM2 method, whereby all myelin is measured. A linear fit to the HM2 data (plotted as a solid line) yields a slope of 0.7 ± 0.1, R = 0.75, $P <$ 0.0001. Comparing the two methods reveals that the size of the short T_2 component is in better agreement with the results of the color-intensity-based approach (HM2), which measured all myelin in a sample, than with the conventional histomorphometric measurement (HM1) of intact myelin only, especially for cut nerves, which tend to have little or no healthy myelin, but do have myelin present in the form of Wallerian degeneration profiles and myelin debris. There is a near one-to-one correspondence (slope = 0.7 ± 0.1) between short T_2 component size and HM2 for both degenerating and regenerating nerve samples, including cut and crushed samples at all time points postinjury as well as normal controls. These results suggest that the short T_2 component does in fact represent total myelin content (HM2) rather than exclusively healthy myelin content (HM1).

DISCUSSION

Cut and crush injuries to rat sciatic nerve provided a model for studying WD in peripheral nerve and, specifically, microstructural changes including loss of myelin, inflammation, and axonal loss. In cases of complete nerve transection, without repair, these processes are irreversible and lead to complete and permanent degeneration. In less severe cases, such as in the case of a crush injury, initial degeneration is followed by regeneration, characterized by myelination of new axons. The goal of this study was to obtain a quantitative measure of myelin in normal and injured nerve samples and to compare myelin content and MR data in order to evaluate the validity of identifying the short T_2 component with myelin content.

We have found that the size of the short T_2 component correlates with the amount of myelin in neural tissue, indicating that multicomponent T_2 relaxation can be used as a direct measure of the processes of myelination in the peripheral nervous system. However, we have also shown that the short T_2 component reflects *all* myelin within the tissue — both intact myelin and myelin "debris," as measured by HM2. The correlation between short T_2 component size and myelin content was found to be 0.75 ($P <$ 0.0001).

The discrimination of intact vs. degenerating myelin may be possible through examining the changes in other features of the T_2 spectra. In the case of crushed nerves, the process of regeneration accompanied by remyelination is clearly marked by an increase in the short T_2 size. In the case of irreversible degeneration (cut nerves), the myelin T_2 component decreased with loss of myelination.

Moreover, we have identified substantial differences between T_2 spectra of degenerating (cut) vs. regenerating crushed nerves. In both cases, not only did the size of the short T_2 component decrease with respect to normal nerve, but a significant shift in the position of the intermediate T_2 component was also observed. In crushed nerve, position of the intermediate and long components increased with decreasing HM2 and positions decreased upon remyelination. However, in cut nerve no relationship was observed between changes in the amount of myelin and intermediate and long component position. These differences in the properties of the T_2 spectra may be useful in differentiating between injured nerve that has the potential to spontaneously regenerate and nerve that does not. By comparing the size of the myelin component

and the position of the intermediate and long components in injured and normal nerve, and by monitoring any changes in the initial weeks after injury, it should be possible to predict the likelihood of spontaneous regeneration. Steadily increasing intermediate T_2 component position may indicate regeneration, even as myelin content is decreasing, whereas elevated but stable intermediate T_2 component position accompanied by decreased myelin content may suggest that spontaneous regeneration is unlikely. At later stages of degeneration, the position of the intermediate component was similar in cut and crushed nerves but the myelin T_2 component in the crushed nerve was closer to normal than it was initially after injury.

In addition to loss of myelin, the processes of axonal loss and inflammation have also been observed. All of these can affect T_2 relaxation. We have shown previously (11) that in the presence of exchange between myelin and intra-axonal/extra-axonal compartments the process of demyelination can also cause a slight shift of the intermediate/long T_2 components towards longer T_2 values. However, the fact that the size of the short component agrees with histomorphometric assessment of myelin content suggests a slow rate of exchange between myelin and other compartments, since if exchange were fast, the size of the short component would be smaller than the myelin content (11). Demyelination can only be responsible for a shift in position of at most 14%, assuming residence time of water in myelin to be around 160 ms (11), compared to the observed increases of up to 104% for the intermediate component and up to 122% for the long component. Other factors contributing to increased T_2 values may include the increase in extracellular matrix volume, cell membrane disruption (leading to increased exchange between extra- and intracellular water), or inflammation. Quantitative assessment of these concurrent contributions to T_2 behavior is beyond the scope of this study and would require control over more experimental parameters and the application of multiple histopathology techniques.

Finally, some studies (9,12) have suggested identification of the intermediate and long T_2 components with intra-axonal and extracellular water. In the present study, the extracellular volume fraction increased following injury (average increases of 66% in cut nerve and 70% in crushed nerve 1 week postinjury). However, the average increase in size of the intermediate component was only 37% in crushed nerve and 39% in cut nerve and long component size decreased by over 50%. Furthermore, the morphometric volume fraction of the extracellular space ($42 \pm 3\%$) did not correspond to the size of the long T_2 component ($21 \pm 3\%$). On the basis of these observations, we postulate that the intermediate component is due to both inter-axonal and extra-axonal water in full exchange, while the long component represents water associated with connective tissues (epineurium, perineurium). It is also interesting to note that although complete axonal loss was seen in cut nerve samples at advanced stages of degeneration, both the intermediate and long T_2 components were observed in the spectra of these samples. Physical evidence of inflammation, including swelling and the presence of inflammatory cells, was observed in the histopathology sections of the injured nerves; however, this has not been quantitatively assessed. Inflammation was more pronounced in the crushed nerve samples, which also demonstrated a greater shift in intermediate and long T_2 than cut nerves. Detailed immunohistology may provide more quantitative information, although unequal volume fractions of components and the presence of exchange would complicate the analysis.

CONCLUSIONS

Multicomponent T_2 spectra provide quantitative information about the state of regeneration or degeneration of an injured nerve. The size of the short T_2 component correlates very well with the histomorphometrically determined myelin content of normal, degenerating, and regenerating peripheral nerves. The size of the short T_2 component is a good quantitative measure of total myelin content, although it is not a good measure of the amount of intact myelin. Changes in the positions of the intermediate and long T_2 components may reflect inflammation and cell membrane disruption, although further investigation is required to make a definitive statement in this regard. MT and diffusion experiments may help elucidate the mechanisms at work. These results further support the use of quantitative MR techniques, including multicomponent T_2 measurements, for quantitative assessment of demyelination and other microstructural changes associated with nerve damage.

ACKNOWLEDGMENTS

We thank Joyce Chan and Lucy Andrighetti, Department of Anatomic Pathology at Sunnybrook and Women's College Health Sciences Centre, for preparation of histology sections, and Jeffrey Mason for assistance with initial histomorphometry analysis.

REFERENCES

1. Moseley ME, Kucharczyk J, Asgari HS, Norman D. Anisotropy in diffusion-weighted MRI. Magn Reson Med 1991;19:321–326.
2. Dailey AT, Tsuruda JS, Filler AG, Maravilla KR, Goodkin R, Kliot M. Magnetic resonance neurography of peripheral nerve degeneration and regeneration. Lancet 1997;350:1221–1222.
3. Neugroschl C, Von Sohsten S, Doll A, Jacques C, Guiraud-Chaumeil C, Warter JM, Dietemann JL. MR imaging of spinal cord in multiple sclerosis: comparison between turbo-spin echo and turbo-IRM. J Neuroradiol 1998;25:263–267.
4. Guy J, Fitzsimmons J, Ellis A, Beck A, Mancuso A. Intraorbital optic nerve and experimental optic neuritis. Ophthalmology 1991;99:720–725.
5. Nakamura T, Yabe Y, Horiuchi Y, Takayama S. Magnetic resonance myelography in brachial plexus injury. J Bone Joint Surg 1997;79B:764–769.
6. Filler AG, Kliot M, Howe FA, Hayes CE, Saunders DE, Goodkin R, Bell BA, Winn RW, Griffiths JR, Tsudura JS. Application of magnetic resonance neurography in the evaluation of patients with peripheral nerve pathology. J Neurosurg 1996;85:299–309.
7. Britz GW, Haynor DR, Kuntz C, Goodkin R, Gitter A, Maravilla K, Kliot M. Ulnar nerve entrapment at the elbow: correlation of magnetic resonance imaging, clinical, electrodiagnostic, and intraoperative findings. Neurosurgery 1996;38:458–465.
8. Pike GB, de Stefano N, Narayanan S, Francis GS, Antel JP, Arnold DL. Combined magnetization transfer and proton spectroscopic imaging in the assessment of pathologic brain lesions in multiple sclerosis. Am J Neuroradiol 1999;20:829–837.
9. Peled S, Cory DG, Raymond SA, Kirschner DA, Jolesz FA. Water diffusion, T-2, and compartmentation in frog sciatic nerve. Magn Reson Med 1999;42:911–918.

10. Sled JG, Pike GB. Quantitative imaging of magnetization transfer exchange and relaxation properties in vivo using MRI. Magn Reson Med 2001;46:923–932.
11. Stanisz GJ, Kecojevic A, Bronskill MJ, Henkelman RM. Characterizing white matter with magnetization transfer and T_2. Magn Reson Med 1999;42:1128–1136.
12. Wachowicz K, Snyder RE. Assignment of the T_2 components of amphibian peripheral nerve to their microanatomical compartments. Magn Reson Med 2002;47:239–245.
13. MacKay AL, Whitall KP, Adler J, Li DKB, Paty DW, Graeb D. In vivo visualization of myelin water in brain by magnetic resonance. Magn Reson Med 1994;31:673–677.
14. Gareau PJ, Rutt BK, Karlik SJ, Mitchell JR. Magnetization transfer and multicomponent T2 relaxation measurements with histopathologic correlation in an experimental model of MS. J Magn Reson Imag 2000; 11:586–595.
15. Does MD, Gore JC. Compartmental study of T_1 and T_2 in rat brain and trigeminal nerve in vivo. Magn Reson Med 2002;47:274–283.
16. Does MD, Snyder RE. Multiexponential T_2 relaxation in degenerating peripheral nerve. Magn Reson Med 1996;32:207–213.
17. Stanisz GJ, Midha R, Munro CA, Henkelman RM. MR properties of rat sciatic nerve following trauma. Magn Reson Med 2001;45:415–420.
18. Sunderland S. A classification of peripheral nerve injuries producing loss of function. Brain 1951;74:491–516.
19. Buehler MJ, Seaber AV, Urbaniak JR. The relationship of functional return to varying methods of nerve repair. J Reconstruct Microsurg 1990;6:61–69.
20. Midha R, Munro CA, Ang LC. End-organ reinnervation does not prevent axonal degeneration in nerve allografts following immunosuppression withdrawal. Restor Neurol Neurosci 1998;13:163–172.
21. Carr HY, Purcell EM. Effects of diffusion on free precession in nuclear magnetic resonance experiments. Phys Rev 1954;94:630–638.
22. Meiboom S, Gill D. Modified spin-echo method for measuring nuclear relaxation times. Rev Sci Instr 1958;29:688–691.
23. Stanisz GJ, Henkelman RM. Diffusional anisotropy of T_2 components in bovine optic nerve. Magn Reson Med 1998;40:405–410.
24. Whittall KP, MacKay AL. Quantitative interpretation of NMR relaxation data. J Magn Reson 1989;95:134.
25. Romero E, Cuisenaire O, Denef JF, Macq BVC. Automatic morphometry of nerve histological sections. J Neurosci Meth 2000;97:111–122.